1.0

1.1

1.25 1.4 1.6

4.5
5.0
5.5

2.8 2.5
3.2 2.2
3.6
4.0 2.0

1.8

MICROCOPY RESOLUTION TEST CHART
NATIONAL BUREAU OF STANDARDS 1963-A

LEVEL Ⅱ

⑫ 15.2

AFGL-TR-78-0119
⑨ AIR FORCE SURVEYS IN GEOPHYSICS, NO. 388

⑥ **Effects of a Time-Varying Photoelectron Flux on Spacecraft Potential**

⑩ HENRY BERRY GARRETT, CAPT, USAF

⑪
15 May 1978

⑫ 30p.

⑭ AFGL-TR-78-0119,
AFGL-AFSG-388

⑯ 7661   ⑰ 08

SPACE PHYSICS DIVISION   PROJECT 7661
AIR FORCE GEOPHYSICS LABORATORY
HANSCOM AFB, MASSACHUSETTS 01731
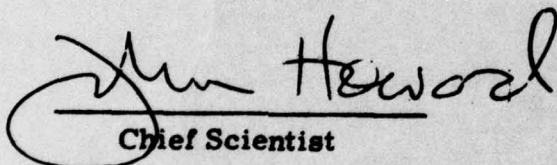
AIR FORCE SYSTEMS COMMAND, USAF

78 09 21 004
409 578

JOB

This report has been reviewed by the ESD Information Office (OI) and is releasable to the National Technical Information Service (NTIS).

This technical report has been reviewed and is approved for publication.

FOR THE COMMANDER

Chief Scientist

Qualified requestors may obtain additional copies from the Defense Documentation Center. All others should apply to the National Technical Information Service.

REPORT DOCUMENTATION PAGE		READ INSTRUCTIONS BEFORE COMPLETING FORM
1. REPORT NUMBER AFGL-TR-78-0119	2. GOVT ACCESSION NO.	3. RECIPIENT'S CATALOG NUMBER
4. TITLE (and Subtitle) EFFECTS OF A TIME-VARYING PHOTOELECTRON FLUX ON SPACECRAFT POTENTIAL		5. TYPE OF REPORT & PERIOD COVERED Scientific. Interim.
		6. PERFORMING ORG. REPORT NUMBER AFSG No. 388
7. AUTHOR(s) Henry B. Garrett, Capt, USAF		8. CONTRACT OR GRANT NUMBER(s)
9. PERFORMING ORGANIZATION NAME AND ADDRESS Air Force Geophysics Laboratory (PHG) Hanscom AFB, Massachusetts 01731		10. PROGRAM ELEMENT, PROJECT, TASK AREA & WORK UNIT NUMBERS 62101F 76610801
11. CONTROLLING OFFICE NAME AND ADDRESS Air Force Geophysics Laboratory (PHG) Hanscom AFB, Massachusetts 01731		12. REPORT DATE 15 May 1978
		13. NUMBER OF PAGES 31
14. MONITORING AGENCY NAME & ADDRESS(if different from Controlling Office)		15. SECURITY CLASS. (of this report) Unclassified
		15a. DECLASSIFICATION/DOWNGRADING SCHEDULE

16. DISTRIBUTION STATEMENT (of this Report)

Approved for public release; distribution unlimited.

17. DISTRIBUTION STATEMENT (of the abstract entered in Block 20, if different from Report)

18. SUPPLEMENTARY NOTES

19. KEY WORDS (Continue on reverse side if necessary and identify by block number)

Satellite anomalies
Spacecraft charging
Plasma interactions

20. ABSTRACT (Continue on reverse side if necessary and identify by block number)

Analysis of plasma data from the geosynchronous satellites ATS-5 and ATS-6 shows that the satellites vary rapidly in potential as they pass into and out of the earth's shadow. These variations result from the loss of photo-electrons as the sun is eclipsed. A model of this phenomenon which includes the effects of atmospheric attenuation of the solar flux between 1000 Å and 3000 Å and spacecraft charge buildup is used to predict the potential variations observed by ATS-5 and ATS-6. The model predicts potentials within ±700 V of the observed potentials in the range -100 V to -10,000 V.

78 09 21 004

Preface

Drs. Hinteregger, Swider, Hardy, Burke, Rothwell, and Rubin provided useful comments and criticism. C. Pike and L. Weeks both contributed pertinent suggestions. Dr. S. DeForest kindly provided the ATS-5 and ATS-6 data, the charging model, and much useful advice. Ms. R. Sagalyn provided the INJUN 5 data. Finally, I appreciate the considerable sacrifices my wife endured by letting me work undisturbed at home.

Contents

Illustrations

5

Effects of a Time-Varying Photoelectron
Flux on Spacecraft Potential

1. INTRODUCTION

Although the potential between a satellite and the ambient plasma is usually on the order of a few volts, the potential can increase to values as high as -18,000 V on time scales of a few minutes as the satellite passes in and out of the earth's shadow. *During such periods, increased arcing occurs.*[1] For this reason, an understanding of the processes involved in these rapid potential variations is of real and immediate interest to spacecraft designers. The purpose of this report is to present a model of these variations.

In order to model the potential variations experienced by a spacecraft as it enters or exits the earth's shadow, it is necessary to estimate the changes in the solar illumination of the spacecraft. This allows the determination of the photo-electron current variations and the resulting potential variations. In the first part of the report a model of the atmospheric attenuation of the solar illumination is developed. In a previous study a model capable of estimating satellite potentials given the ambient and photoelectron currents was derived. This model is combined with the attenuation model to estimate the varying spacecraft potential. The pre-dicted potentials are then compared with the actual data. The results of this

1. Shaw, R.R., Nanevicz, S.E., and Adamo, R.C. (1976) Observations of elec-trical discharges caused by differential satellite charging, AIAA Progress in Astronautics and Aeronautics, A. Rosen (ed.), 47:61-76.

comparison indicate a standard deviation of approximately ±700 V between the predicted and observed values. The FORTRAN programs for the model are included in Appendix A.

2. SATELLITE OBSERVATIONS

Three different satellites served as data sources for the study. The geosynchronous satellites ATS-5 and ATS-6 were the principal sources for data on the ambient plasma environment and on the satellite potential, while the polar-orbiting, low-altitude INJUN 5 satellite provided information on the photoelectron current. The reader is referred to DeForest and McIlwain[2] for details of the ATS-5 instrument, Mauk and McIlwain[3] for the ATS-6 instrument, and Burke et al[4] for the INJUN V instrument.

The ATS-5 and ATS-6 satellites are in low inclination, geosynchronous orbits. The ATS-5 satellite is cylindrical (1.8 m long by 1.5 m in diameter). It spins at 1.27 rps with its axis parallel to the earth's rotation axis. ATS-6, in contrast, is essentially a large (10 m) spin-stabilized dish antenna. The plasma data were obtained from the University of California at San Diego (UCSD) plasma experiments on ATS-5 and ATS-6. Both instruments consist of electrostatic analyzers designed to measure the positive ion and electron populations between 51 eV and 51 keV for ATS-5 and between 0 and 80 keV for ATS-6.

The ATS-5 and ATS-6 instruments measure the particle flux in 64 channels (2 background channels and 62 energy channels), returning a complete energy spectrum in roughly 15 to 20 seconds. For ATS-5, the center energy for a channel is 112 percent of the center energy of the previous channel. For ATS-6 this value is ~113 percent. This results in an uncertainty of about ±5 percent in the energy (or potential) determination.

The ATS-5 and ATS-6 instruments return count rate data which are converted to differential energy spectra. From the differential energy spectra, the ambient currents and distribution functions necessary in estimating the satellite potential are determined. The satellite spectra also indicate the spacecraft potential. Briefly, the low energy ion (electron) population is accelerated if the satellite has a negative (positive) potential relative to the ambient plasma. This acceleration produces a pronounced peak in the low energy ion (electron) channels at an energy in electron volts (eV) corresponding to the satellite potential in volts (V). Thus, ATS-5 and

2. DeForest, S. E., and McIlwain, C. E. (1971) Plasma clouds in the magnetosphere, J. Geophys. Res., 76(No. 16):3587-3611.

3. Mauk, B. H., and McIlwain, C. E. (1975) ATS-6 UCSD Auroral Particles Experiment, IEEE Trans. Aerospace and Electronic Systems, AEA-11(No. 6); 1125-1130.

4. Burke, W. J., Donatelli, D. E., and Sagalyn, R. C. (1978) INJUN 5 observations of low-energy plasma in the high-latitude topside ionosphere, to appear in J. Geophys. Res.

ATS-6 provide information on both the ambient plasma and the spacecraft potential. The 25 eclipse passages for which these quantities were determined are listed in Table 1.

Table 1. Date and Approximate Start and End Time (UT) of ATS-5 and ATS-6 Eclipses. Potentials immediately following entry and preceding exit from eclipse

ATS-5	Eclipse Passages			
Date	Entry	Potential	Exit	Potential
22 Sep 1969	0628	-3404	0732	-3810
16 Oct 1969	0626	-5357	0712	-3810
12 Sep 1970	0630	-2423	0719	-1730
15 Sep 1970	0625	-877	0722	-1539
17 Sep 1970	0622	-5378	0723	-3041
19 Sep 1970	0620	-2725	0724	-1939
26 Sep 1970			0725	-2168
5 Oct 1970	0615	-5357	0719	-3811
17 Oct 1970	0628	-1232	0700	-2172
18 Oct 1970	0632	-397	0655	-316
19 Oct 1970	0638	-558	0649	-558
ATS-6				
28 Feb 1976	2143	-9330	2200	-8140
6 Mar 1976	2124	-7110	2219	-9330

The INJUN 5 satellite is a magnetically-aligned, polar-orbiting satellite with a spin period of 20 min, an inclination of 81°, an apogee of 2453 km, and a perigee of 677 km. Data were used from the Air Force Geophysics Laboratory (AFGL) spherical electrostatic analyzers (SEA). These analyzers consist of a spherical tungsten collector surrounded by two concentric wire mesh grids. The current to the collector grid is measured at 3 or 40 samples per second. When the ion collector is illuminated, the resulting photoelectron flux is the dominant source of the measured current. As the spacecraft approaches the earth's shadow, the photoelectron flux decreases in response to atmospheric attenuation. As will be discussed, this will allow a calibration of the atmospheric attenuation model.

3. ATMOSPHERIC ATTENUATION

Theory and observation indicate a linear relation between the photon flux falling on a surface and the photoelectron flux emitted by that surface. As a satellite passes into eclipse, the percentage of the solar disk that is visible decreases. The percentage decrease in the visible solar disk is equal to the percentage change in the photon flux. Given an estimate of the percent attenuation of the solar disk and of the total photoelectron current for the unattenuated solar disk, it is straightforward to calculate the changing photoelectron currents. In this section we estimate the attenuation of the solar disk. In Section 5 we will determine the total photoelectron current.

The problem of finding the percentage of the solar disk that is obscured as the satellite passes into the earth's shadow has two parts—determination of the position of the center of the solar disk and determination of the atmospheric attenuation. The two operations can be treated separately if the concept of X_m, the minimum ray path altitude, is introduced. X_m (Figure 1) is defined as the minimum distance from the earth that a ray of light travels in going from the center of the sun to the satellite. The problem of finding the percentage of the solar disk that is obscured reduces to that of finding the atmospheric attenuation as a function of X_m and finding X_m, as seen from the satellite, as a function of time or position in orbit.
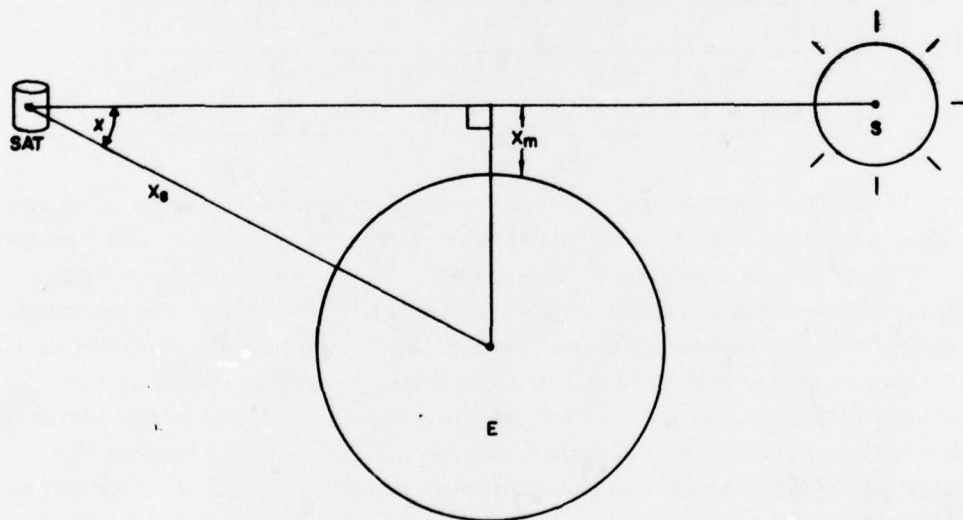
Figure 1. Illustration of the Meaning of χ, the Angle Between the Sun (S) and the Earth's (E) Center, X_s, the Distance From the Satellite (SAT) to the Center of the Earth, and X_m, the Minimum Ray Path

10

3.1 Determination of X_m

X_m is determined as a function of satellite-earth-sun position in spherical coordinates. Step one is the determination of the angle, χ, between the center of the earth and the sun-satellite line (see Figure 2). χ is a function of the latitude of the sun ($\delta_\odot$) and the satellite (δ_s) relative to the earth and the longitude of the sun ($\alpha_\odot$) and the satellite (α_s) (Figure 3). The sun is considered to be at infinity so that the longitude and latitude of the sun relative to a coordinate system based on the earth-mean sun (or satellite-mean sun) line and the spin axis of the earth are equal for the earth and satellite. Thus, the latitude of the sun in the satellite coordinate system is (Figure 3a)

$$\delta_\odot(\text{sat}) = \delta_\odot(\text{earth}) . \tag{1}$$
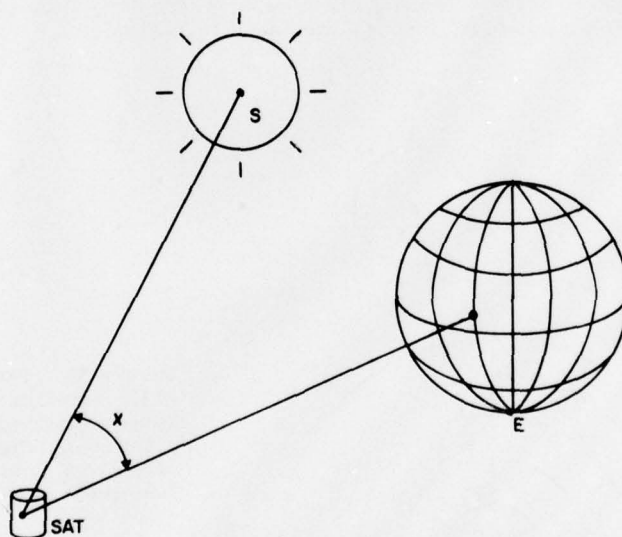
Figure 2. Detail of the Measurement of the Angle χ (S - SAT - E)

The latitude of the earth ($\delta_\oplus$) in the satellite system becomes (Figure 3b)

$$\delta_\oplus(\text{sat}) = -\delta_s(\text{earth}) . \tag{2}$$

11
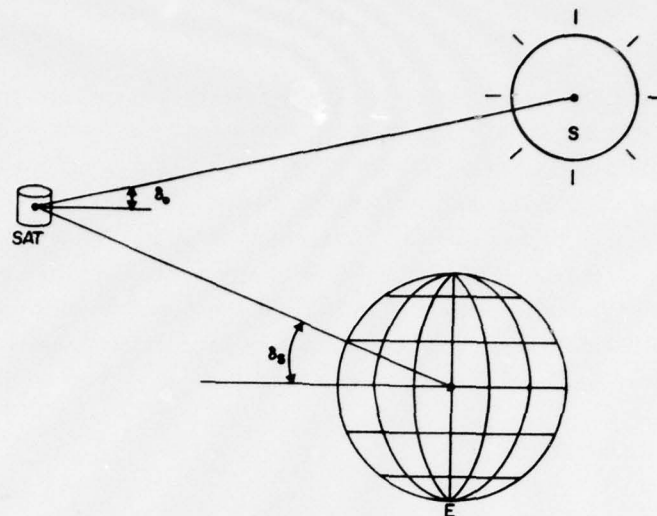
Figure 3a. Meridian Projection of the Satellite-Sun-
Earth System Showing the Measurement of $\delta_\odot$, the
Solar Latitude, and δ_s, the Satellite Latitude
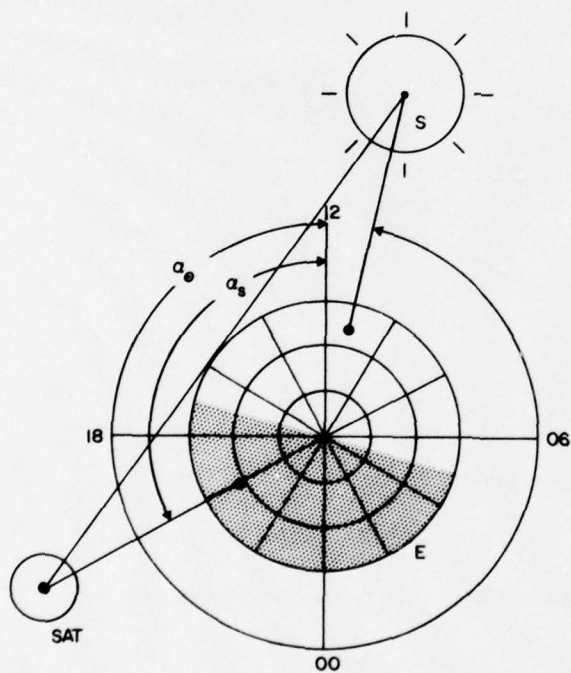
Figure 3b. Polar Projection
of the Satellite-Sun-Earth
System Showing the Measure-
ment of $\alpha_\odot$, the Longitude
of the Sun, and α_s, the
Longitude of the Satellite

12

If longitude is reckoned in the same direction from mean local noon in the satellite and earth systems (remember, as the sun is at infinity, the satellite-mean sun and earth-mean satellite sun lines are parallel), then the longitude of the sun in the satellite system is

$$\alpha_{\odot}(\text{sat}) = \alpha_{\odot}(\text{earth}) . \tag{3}$$

Likewise, the longitude of the earth's center in the satellite coordinate system is

$$\alpha_{\oplus}(\text{sat}) = \alpha_{s}(\text{earth}) - 180° . \tag{4}$$

Thus, the separation in longitude of the sun's center and the earth's center as seen from the satellite is

$$\alpha = \alpha_{\oplus}(\text{sat}) - \alpha_{\odot}(\text{sat})$$

$$= (\alpha_{s}(\text{earth}) - 180°) - \alpha_{\odot}(\text{earth}) . \tag{5}$$

We now have the latitudes of the sun and earth in terms of the satellite coordinate system and their relative displacement in longitude. Referring to Figure 4, the problem reduces to solving a spherical triangle, the solution of which is

$$\cos \chi = \cos (90° - \delta_{\odot}) \cos (90° - \delta_{\oplus})$$

$$+ \sin (90° - \delta_{\odot}) \sin (90° - \delta_{\oplus}) \cos \alpha$$

$$= \sin (\delta_{\odot}) \sin (\delta_{\oplus}) + \cos (\delta_{\odot}) \cos (\delta_{\oplus}) \cos \alpha . \tag{6}$$

Once χ is given, X_m follows immediately (Figure 1)

$$X_m = XS \cdot \sin (\chi) - R_E , \tag{7}$$

where

XS = distance from earth to satellite (in km) ,

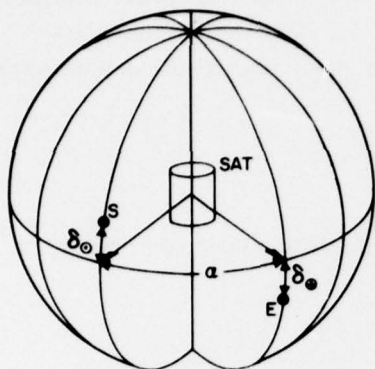R_E = radius of earth (6378 km) .

13

Figure 4. Illustration of the Actual
Spherical Trigonometric Problem in
Terms of the Satellite Reference System

3.2 Determination of Atmospheric Attenuation

The determination of atmospheric attenuation is uncertain since the exact re-
sponse of satellite materials to solar flux is not well known so that the wavelength
ranges of interest are not well defined. Also, the apparent size of the sun varies
slightly with wavelength and with solar activity (prominences and the corona can
introduce asymmetries in the shape of the sun at ultraviolet wavelengths). Further,
the atmosphere itself varies in time. The best solution at present is an
iterative process in which each of the unknowns is varied within a reasonable
range.

The process of determining atmospheric attenuation has three steps. First,
a model of the attenuation of the atmosphere is assumed. Secondly, the attenuation
factor is integrated over the disk of the sun. This is done for the required values
of X_m to give a table of percent illumination (assumed to be directly proportional
to photoelectron current) vs X_m. In the third step, to be carried out in a later
section, the results are compared with a plot of the photoelectron current required
to give the observed potentials as a function of X_m. The atmospheric model and
total photoelectron current are varied until agreement is reached.

The satellites' response curves are assumed to be similar to that of aluminum
so that only the wavelength range between ~ 1000 Å and ~ 3000 Å is significant. This
means only ultraviolet radiation will be considered. The cross-section for absorp-
tion is, in general, orders of magnitude larger than scattering at these wavelengths
so the radiation is attenuated long before significant scattering or refraction takes
place. Likewise, in the altitude range over which significant attenuation is ex-
pected, O_2 and O_3 are the dominant absorbing species. The altitude (30 to 90 km)
where these species absorb most of the flux is little affected by latitude or geo-
magnetic effects.

14

For an atmosphere which falls off exponentially in altitude, the photon flux ϕ as a function of wavelength and X_m for a single constituent is

$$\phi(\lambda, X_m) = \phi_\infty(\lambda) e^{-\tau} \tag{8}$$

where

$$\tau = n(X_m) \sigma_a (2\pi R_e H)^{1/2},$$

R_e = earth's radius,

$n(X_m)$ = number density,

H = scale height of constituent at X_m,

$\phi_\infty(\lambda)$ = unattenuated solar flux at wavelength λ,

σ_a = absorption cross section at wavelength λ.

For simplicity, an exponential atmosphere is assumed

$$n(X_m) = n_o e^{\frac{-(X_m - X_o)}{\delta X}},$$

n_o, X_o, δX constants for given constituent.

Then

$$\phi(X_m, \lambda) = \phi_\infty(\lambda) e^{-e^{\frac{-(X_m - Z_o)}{\delta Z}}} \tag{9}$$

where all the constants have been lumped into Z_o and δZ.[5]

Neither the O_2 or O_3 density follows a strictly exponential curve in the region of interest. The apparent diameter of the sun, however, is 370 km as viewed by a satellite at geosynchronous orbit. Thus, a gross averaging will take place such that wavelength and scale height variations are smoothed out if the attenuation is considered for the entire solar disk. To first order, a model of atmospheric attenuation of the functional form given in Eq. (9) should be adequate.

Once the attenuation function in terms of X_m is assumed, an integration over the disk of the sun can be performed. Again, the calculation is carried out in spherical coordinates. Previously $\chi(X_m)$, the angular separation between the center of the solar disk (assumed to be the optical center) and the center of the earth, was

5. Swider, W. (1964) The determination of the optical depth at large solar zenith distance, Planet. Space Sci. 12:761-782.

determined. In conjunction with XS, the distance from the satellite to the center of the earth, the value of the total flux (ϕ_T) as a function of X_m becomes

$$\phi_T \, (X_m) = \int_0^{\alpha_{r\odot}} d\theta \int_0^{2\pi} [\phi'(\theta,\varphi) \, \sin(\theta)] \, d\varphi \, , \qquad (10)$$

where

$$\phi'(\theta,\varphi) = \phi_\infty \, e^{-e^{\frac{-(X-Z_o)}{\delta Z}}} \, ,$$

$$X = XS \cdot \sin(\chi') - R_e \, ,$$

$$\chi' = \cos^{-1}(\cos(\theta)\cos(\chi) + \sin(\theta)\sin(\chi)\cos(\varphi)) \, ,$$

$\alpha_{r\odot}$ = angular radius of sun (function of day of year) ,

$\phi_\infty, \, Z_o, \, \delta Z$ = assumed constants for atmospheric model .

The geometry is illustrated in Figure 5. The percentage of solar flux, $P(X_m)$, is given by dividing $\phi_T \, (X_m)$ by $\phi_T \, (\infty)$. As $\phi'(\theta,\varphi)$ goes to ϕ_∞ as X_m goes to infinity, this gives

$$P(X_m) = \frac{\phi_T(X_m)}{\phi_T(\infty)} = \frac{\phi_T(X_m)}{\phi_\infty \, 2\pi \, (1-\cos(\alpha_{r\odot}))} \, . \qquad (11)$$
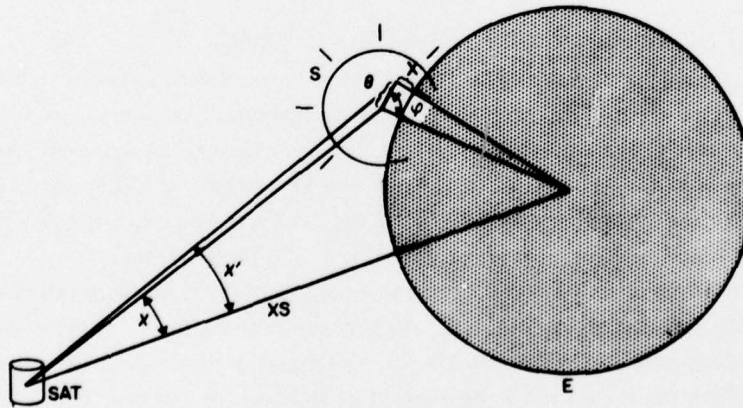
Figure 5. Geometric Representation of the Obscurations of the Solar Disk Upon Eclipse Entry. The variables are defined in the text

16

As discussed earlier, INJUN V data provide an estimate of $P(X_m)$. In Figure 6, $P(X_m)$ is plotted for the INJUN V satellite for the case of no atmosphere (complete attenuation below $X_m = 0$ km), for an atmospheric model having $Z_o = 90$ km and $\delta Z = 40$ km, and for an O_3 atmosphere ($\delta Z \sim 4.67$ km, $Z_o \sim 76.4$).[6] Also shown is the percentage of photoelectron current measured as the satellite was eclipsed. Even though INJUN 5 is at 2500 km altitude where the attenuation should readily show the effects of atmospheric variations, the simple model (assuming
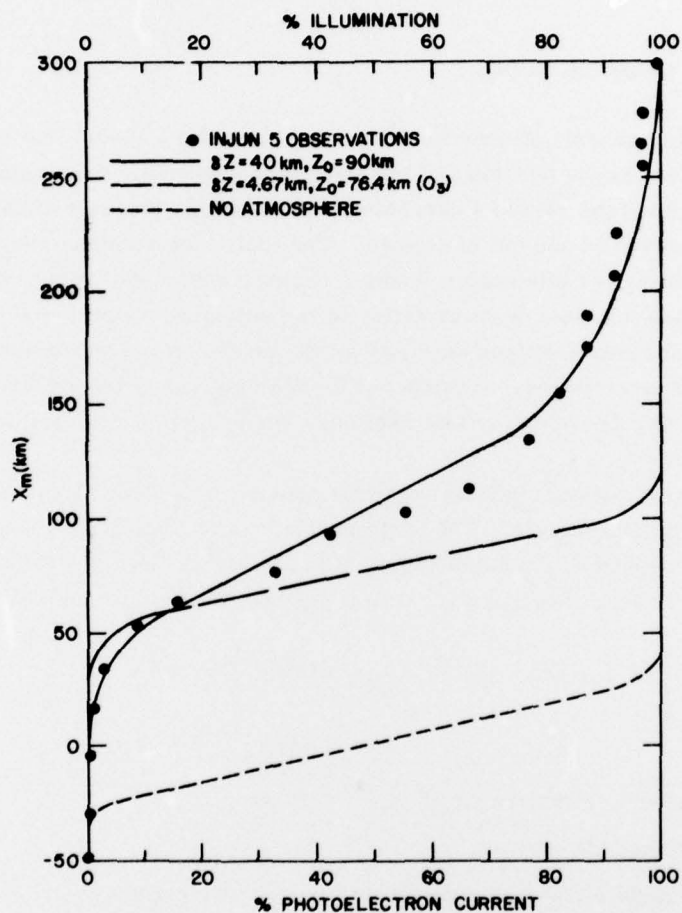
Figure 6. Percentage of the Solar Illumination Reaching the Spacecraft and the Percentage of Photoelectron Current Measured by INJUN 5 as Functions of X_m, the Minimum Ray Path Altitude

6. Weeks, L. H., Cuikay, R. S., and Corbin, J. R. (1972) Ozone measurements in mesosphere during the solar proton event of 2 November 1969, J. Atmos. Sci., 29(No. 6):1138-1142.

17

Z_o = 90 km and δZ = 40 km) is adequate, demonstrating the smoothing over wavelength and height. In lieu of knowledge of the photo-emission response functions for the ATS-5 and ATS-6 satellites, the INJUN 5 (or tungsten) attenuation function (δZ = 40 km and Z_o = 90 km) will be assumed. We will, however, compare the results for this assumption with those for no atmosphere. At geosynchronous orbit, the difference between the two assumptions is not as great as implied by Figure 6. Also, the INJUN 5 attenuation function gives adequate results over the X_m range of interest and, unlike other functions that might be assumed, is based on observational data.

4. SPACECRAFT CHARGING MODEL

Given the atmospheric attenuation function we require a model that predicts potential variations in the presence of photoelectron currents. This model will be needed in calculating the residual current—presumably the photoelectron current—as the spacecraft passes in and out of eclipse. The total photoelectron current will be determined by fitting the attenuation function to these residuals. Given this value and the attenuation function, we may estimate the potential variations as the spacecraft passes in and out of eclipse—the goal of the study. A model capable of calculating spacecraft potentials as a function of the ambient currents and meeting these objectives is briefly presented in this section. The reader is referred to Garrett[7] for more details.

The problem of determining the potential between a spacecraft and the ambient plasma is conceptually simple. The basic problem is to find, for a given set of ambient plasma conditions, a satellite potential for which there is 0 net current to the spacecraft surface. Specifically, it is necessary to find V such that

$$J_e(V) - (J_I(V) + J_{se}(V) + J_{SI}(V) + J_{BS}(V) + J_{ph}(V)) = 0 , \tag{12}$$

where

J_e = incident electron current,

J_I = incident ion current,

J_{se} = secondary electron current emitted by incident electrons,

J_{SI} = secondary electron current emitted by incident ions,

J_{BS} = backscattered electron current,

J_{ph} = photoelectron current.

7. Garrett, H.B. (1978) Spacecraft Potential Calculations - A Model, AFGL-TR-78-0116.

18

The currents are all functions of the ambient particle distributions and satellite potential, V. Their calculation, in terms of the ATS-5 and ATS-6 UCSD plasma data, is described in Garrett.[7] Given these currents, the potential is determined by an iterative procedure in which V is varied until Eq. (12) holds.

The ratios of the secondary and backscattered currents to the ambient current are not known accurately. Likewise, the photoelectron current is not known. It is necessary, therefore, to initially "calibrate" the potential model. This is done by first choosing particle spectra immediately before (immediately after) and immediately after (immediately before) the spacecraft pass into (out of) the earth's shadow (see Table 1). The photoelectron current is assumed to be 0 and the secondary and backscattered ratios adjusted until the predicted potentials agree with the observed potentials in a least squares sense. The results of this procedure for the ATS-5 and ATS-6 satellites are presented in Figure 7.
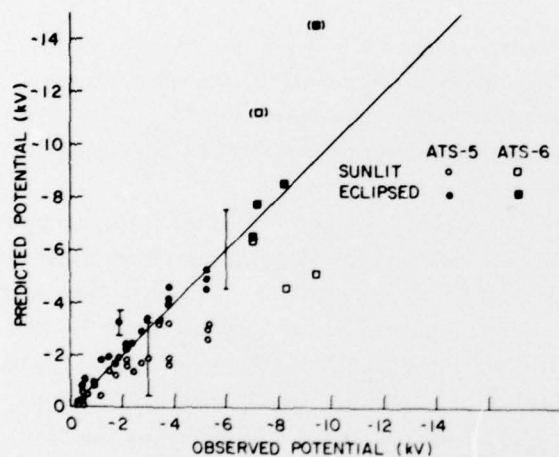
Figure 7. The Predicted and Observed Potentials for ATS-5 and ATS-6 for Total Eclipse of the Sun. The closed symbols are for values calculated using the eclipsed spectra. Open symbols are for values calculated using the sunlit spectra

The error bars in Figure 7 correspond to a ± 1σ deviation. For the entire data set (both sunlit and eclipsed spectra), the error bar is ± 1500 volts. Ignoring the two outlying points (the plasma changed significantly during eclipse passage for these points), the error is ± 1300 V for the sunlit spectra and ± 500 V for the eclipsed spectra.

The difference between the predictions due to the sunlit and eclipsed spectra is believed to result from the lack of knowledge about the particles outside the detector's energy range and from the finite interval (particularly at high energies) between energy steps. Shifting the sunlit spectra in energy to account for the satellite potential accentuates these problems. A similar difficulty arises when the eclipsed

19

spectra are shifted down in potential. Thus, an error of about 25 percent is introduced that is dependent on satellite potential. Although spectra taken at the same time as the desired potential calculation are clearly to be preferred, it is not possible to do this in most cases. In the discussions that follow, the results presented will either be the average of the eclipsed and sunlit spectra or designated as sunlit and eclipsed estimates.

In summary, given the ambient plasma distribution, the currents to the spacecraft can be estimated as a function of satellite potential. Given the currents as functions of spacecraft potential, the spacecraft potential can be calculated. It is necessary, however, to "calibrate" the secondary and backscattered currents. This was done for eclipse conditions when the photoelectron current was zero. The model can then be used to estimate the residual (photoelectron) currents as the spacecraft is eclipsed or to estimate satellite potentials.

5. RESULTS

As discussed in the previous sections, we need to determine the total ATS-5 and ATS-6 photoelectron currents. Once given these currents, the atmospheric attenuation function gives the photoelectron current as a function of X_m. Knowing the ambient conditions, we then calculate the spacecraft potential as a function of X_m.

To determine the total ATS-5 and ATS-6 photoelectron currents, the spacecraft charging model is used to estimate the residual current—that is, the current necessary to give the observed potential after all known currents are accounted for—as a function of X_m. In Figures 8a and 8b we have plotted these currents (actually the number fluxes). Shown for both satellites are the INJUN V atmospheric attenuation function and the attenuation function for no atmosphere. The attenuation functions have been fit to the data. In the case of ATS-5, the INJUN 5 function fits the observed fluxes quite well, while for no atmosphere the function does not fit values having an X_m of 0 or greater. For ATS-6, it is not possible to unambiguously choose either function. The total photoelectron fluxes implied by these fits are, in number/cm^2-sec-ster

	ATS-5	ATS-6
No Atmosphere	5×10^7	1.2×10^8
(Z_o = 90 km, Z - 40 km)	2.5×10^8	4.0×10^8

20

Figure 8a. The Residual (Photoelectron) Current Estimated for 21 ATS-5 Eclipse Passages. This is the current necessary to explain the observed satellite potential after all ambient and secondary currents have been subtracted. Two atmospheric attenuation profiles are also plotted
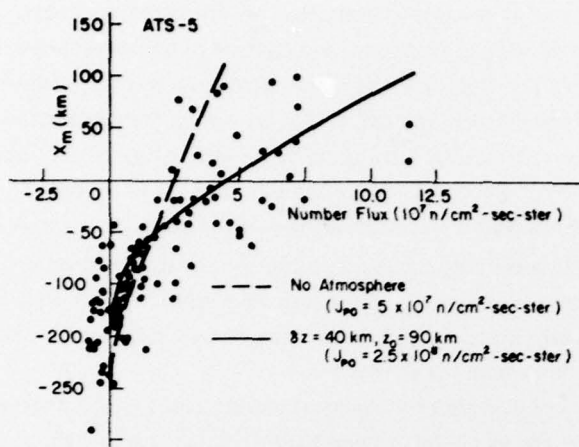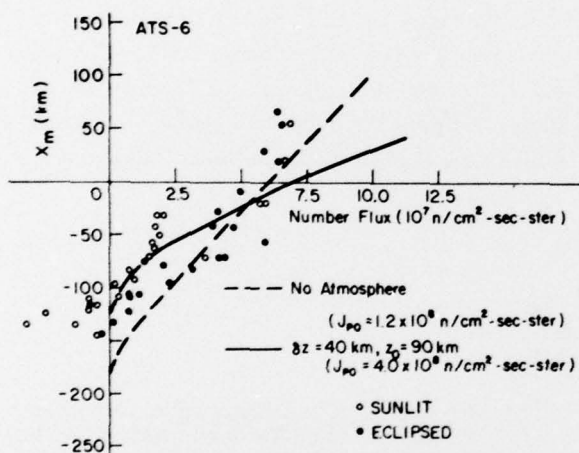

Figure 8b. The Residual (Photoelectron) Current Estimated for 4 ATS-6 Eclipse Passages. This is the current necessary to explain the observed satellite potential after all ambient and secondary currents have been subtracted. Two atmospheric attenuation profiles are also plotted

For ATS-5, these values can be converted directly to currents by multiplying by the total spacecraft area $(1.8 \times 10^5 \text{ cm}^2)$, dividing by the sunlit cross-section $(\sim 2.7 \times 10^4 \text{ cm}^2$ for the side), and multiplying by πq (q is charge). The ATS-5 fluxes give 0.552 nA/cm^2 and 0.11 nA/cm^2. Grard et al[8] predict currents on the order of 0.4 nA/cm^2 (graphite) to 4.2 nA/cm^2 (aluminum oxide). Thus the INJUN 5 attenuation factor gives low but reasonable values for the total photoelectron current. Considering the complex ATS-6 geometry, it is not possible to accurately calculate the current.

8. Grard, R.J.L., Knott, K., and Pedersen, A. (1973) The influence of photo-electron and secondary electron emission on electric field measurements in the magnetosphere and solar wind, Photon and Particle Interactions with Surfaces in Space, R.J.L. Grard (ed.), pp 163-189.

The major source of errors in the preceding calculation is the satellite orbit. Although the calculation of the orbit of a geosynchronous satellite is straightforward since relatively few perturbations occur, the satellite ephemerides are only updated on a 2 or 3 week basis. All of the orbital periods studied were 4- to 7-day extrapolations. Errors, particularly in the time of local midnight, on the order of ~10 sec were typical for ATS-5, while the error in the ATS-6 ephemerides were on the order of 90 seconds. Such errors translate to errors on the order of ± 15 km and ± 150 km in X_m. It was necessary to assume eclipse symmetry around midnight and adjust the time of local midnight accordingly. Although this significantly improved individual eclipse pairs (particularly for ATS-6), errors in latitude of ± 0.05° (corresponding to errors in X_m of 35 km or less) remain.

Given the INJUN 5 attenuation function and the corresponding total photoelectron current we use Eq. (12) to calculate the spacecraft potential as a function of the ambient plasma conditions.

Figures 9, 10, and 11 represent the end product of this analysis. In Figure 9, the voltage prediction for the 25 eclipse passages listed in Table 1 (~230 potential observations) have been plotted vs observed values for ATS-5 and ATS-6. The standard deviation set is ± 700 volts. Error bars of ± 500 V are shown. In Figures 10 and 11 four different eclipse passages are plotted to give an idea of the power of the technique. The bars for the predicted values correspond to the eclipsed (upper) and sunlit (lower) predictions.
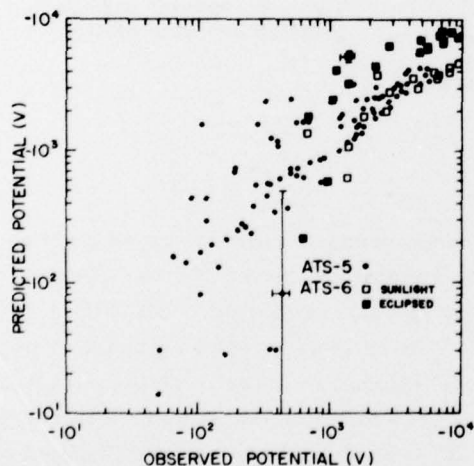
Figure 9. The Observed and Predicted Potentials for ATS-5 and ATS-6 for the Entire Data Base. The values for ATS-5 are the averages of the sunlit and eclipsed spectra. For ATS-6 the different spectra are indicated

22
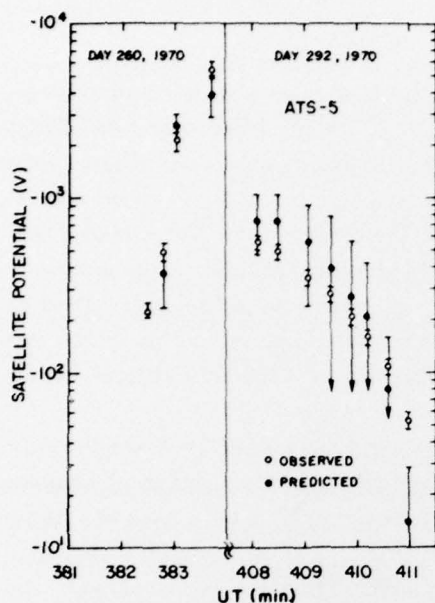
Figure 10. The Observed and Predicted
(average of the sunlit and eclipsed spectra)
Potentials for the Eclipse Entry of ATS-5
on Day 260, 1970 and for Eclipse Exit on
Day 292, 1970

Figure 11. The Observed and Predicted
(average of the sunlit and eclipsed spectra)
Potentials for the Eclipse Entry of ATS-6
on Day 66, 1976 and Eclipse Exit on
Day 69, 1976

23

6. CONCLUSIONS

The detailed calculation of the effects of a time-varying photoelectron flux on spacecraft potential has hinged on the concept of X_m, the minimum ray path altitude. Use of this parameter allowed the division of the calculation into three steps. First, an atmospheric attenuation function was derived as a funct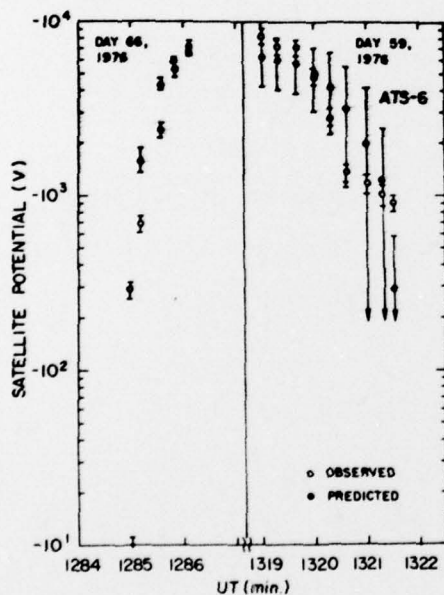ion of X_m. Next, following the calibration of the secondary and backscattered flux ratios, the residual flux (the photoelectron current) as a function X_m was calculated for the entire set of data. Finally, the total photoelectron flux was determined for ATS-5 and ATS-6 by fitting the atmospheric attenuation function to the data. Using this value it was then possible to estimate the spacecraft potential variations as a function of time-varying photoelectron flux.

The implications of the model are obvious. For ATS-5 and ATS-6 the model can predict the range of charge buildup as the spacecraft move in and out of eclipse and provide important information for spacecraft designers. The effects of a time-varying current source (the photoelectron current) on spacecraft potential can be studied. The model also evaluates the accuracy of the simple charge-balance model[7,9] presented in Section 4. Though not discussed, the effects of neglecting the plasma sheath surrounding the spacecraft can be evaluated. In the final analysis, the major importance of the model is that it can be used to evaluate the interaction between the ambient environment and the spacecraft under commonly occurring conditions at geosynchronous orbit. It is to this end that this study was instigated.

9. DeForest, S. E. (1972) Spacecraft charging at synchronous orbit, J. Geophys. Res., 77(No. 4):651.

24

References

1. Shaw, R.R., Nanevicz, S.E., and Adamo, R.C. (1976) Observations of electrical discharges caused by differential satellite charging, AIAA Progress in Astronautics and Aeronautics, A. Rosen (ed.), 47:61-76.

2. DeForest, S.E., and McIlwain, C.E. (1971) Plasma clouds in the magnetosphere, J. Geophys. Res., 76(No. 16):3587-3611.

3. Mauk, B.H., and McIlwain, C.E. (1975) ATS-6 UCSD Auroral Particles Experiment, IEEE Trans. Aerospace and Electronic Systems, AEA-11(No. 6): 1125-1130.

4. Burke, W.J., Donatelli, D.E., and Sagalyn, R.C. (1978) INJUN 5 observations of low-energy plasma in the high-latitude topside ionosphere, to appear in J. Geophys. Res.

5. Swider, W. (1964) The determination of the optical depth at large solar zenith distance, Planet. Space Sci., 12:761-782.

6. Weeks, L.H., Cuikay, R.S., and Corbin, J.R. (1972) Ozone measurements in mesosphere during the solar proton event of 2 November 1969, J. Atmos. Sci., 29(No. 6):1138-1142.

7. Garrett, H.B. (1978) Spacecraft Potential Calculations - A Model, AFGL-TR-78-0116.

8. Grard, R.J.L., Knott, K., and Pedersen, A. (1973) The influence of photo-electron and secondary electron emission on electric field measurements in the magnetosphere and solar wind, Photon and Particle Interactions with Surfaces in Space, R.J.L. Grard (ed.), pp 163-189.

9. DeForest, S.E. (1972) Spacecraft charging at synchronous orbit, J. Geophys. Res., 77(No. 4):651.

The FORTRAN programs designed to calculate the atmospheric attenuation
function will be briefly described. Listings are provided following this section. It
will be assumed that, as input, one has available

RC = angular distance in radians between center of earth and
sun-satellite line,
[χ in Eq. (10)]

RE = radius of earth in R_e,

RS = angular radius of sun in radians [$\alpha_{r\odot}$ in Eq. (10)],

XS = distance, in R_e, from satellite to center of earth
[XS in Eq. (10)] .

The subroutine will return:

AILL = Area illuminated or percent of unattenuated solar flux
[$P(X_m)$ in Eq. (11)] .

Also required is an atmospheric attenuation model as a function of altitude above
the earth's surface, X. A model of the form given in Eq. (9) is assumed here. Z0
and DZ (Z_o and δZ) are in COMMON/ATMOS/.

Given RC, RE, RS, and XS, the subroutines calculate AILL by means of Eq.
(10) which is a double integral over $d\theta$ and $d\varphi$. The variables in the subroutine
correspond to the parameters in Eq. (10) as follows

27

$$F \leftrightarrow [\phi'(\varphi) \sin \theta],$$
$$AA \leftrightarrow \chi'$$
$$DTH \leftrightarrow d\varphi,$$
$$THT \leftrightarrow \varphi,$$
$$DR \leftrightarrow d\theta,$$
$$R \leftrightarrow \theta.$$

The basic program calls are structured as follows
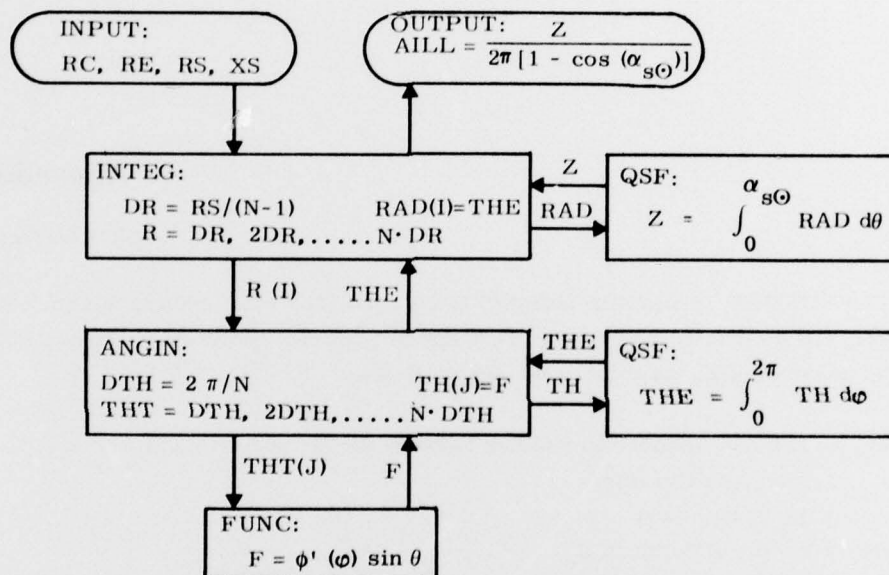
N is the step size. In the listings shown, N = 10 giving run times of ~0.02 sec/value. For the final run, N = 100 giving run times of ~1.5 sec/value.

The subroutine INTEG, as indicated, finds DR and R(I). In subroutine ANGIN, DTH, and THT(I) are determined. In subroutine FUNC, using R(I) and THT (I), F is found. Given the vector TH(J), it is integrated in QSF to give THE. THE for various values of R(I) are stored in RAD (I). RAD (I) is integrated in QSF to give Z, the amount of the solar disk visible from the satellite.

The subroutine QSF is a standard systems program which takes a vector Y of function values spaced an equal distance H apart. The integrals are returned in another vector Z.

```
      SUBROUTINE INTEG(RC,RE,RS,XS,AILL)
      DIMENSION RAD(100),Z(100)
      DR=RS/9.
      DO 1 I=1,10
      R=DR*FLOAT(I-1)
      CALL ANGIN(R,RC,RE,XS,THE)
    1 RAD(I)=THE
      CALL OSI(DR,RAD,Z,10 )
      AILL=Z(10 )
      RSA=6.28718*(1.-COS(RS))
      AILL=AILL/RSA
      RETURN
      END


      SUBROUTINE FUNC(R,RC,RE,THT,F,XS)
      COMMON/THOS/Z0,DZ
      AA=ACOS(COS(R)*COS(RC)+SIN(R)*SIN(RC)*COS(THT))
      X=XS*SIN(AA)
      X=X-RE
      X=X*6378.
      Z=(X-Z0)/DZ
      ZI=ABS(Z)
      IF(ZI.LT.1.E-08)Z=1.E-08*Z/ZI
      IF(ZI.GT.500.)Z=Z*500./ZI
      Z=EXP(-Z)
      ZI=ABS(Z)
      IF(ZI.GT.500.)Z=Z*500./ZI
      IF(ZI.LT.1.E-08)Z=1.E-08*Z/ZI
      Z=EXP(-Z)
      IF(X.LT.0.)Z=0.
      F=SIN(R)*Z
      RETURN
      END


      SUBROUTINE ANGIN(R,RC,RE,XS,THE)
      DIMENSION TH(100),Z(100)
      DTH=6.28318/9.
      DO 1 I=1,10
      THT=DTH*FLOAT(I-1)
      CALL FUNC(R,RC,RE,THT,F,XS)
    1 TH(I)=F
      CALL OSI(DTH,TH,Z,10 )
      THE=Z(10 )
      RETURN
      END
```

```
C          SUBROUTINE QSF
C
C          PURPOSE
C             TO COMPUTE THE VECTOR OF INTEGRAL VALUES FOR A GIVEN
C             EQUIDISTANT TABLE OF FUNCTION VALUES.
C
C          USAGE
C             CALL QSF (H,Y,Z,NDIM)
C
C          DESCRIPTION OF PARAMETERS
C             H       - THE INCREMENT OF ARGUMENT VALUES.
C             Y       - THE INPUT VECTOR OF FUNCTION VALUES.
C             Z       - THE RESULTING VECTOR OF INTEGRAL VALUES. Z MAY BE
C                       IDENTICAL WITH Y.
C             NDIM    - THE DIMENSION OF VECTORS Y AND Z.
C
C          REMARKS
C             NO ACTION IN CASE NDIM LESS THAN 3.
C
C          SUBROUTINES AND FUNCTION SUBPROGRAMS REQUIRED
C             NONE
C
C          METHOD
C             BEGINNING WITH Z(1)=0, EVALUATION OF VECTOR Z IS DONE BY
C             MEANS OF SIMPSONS RULE TOGETHER WITH NEWTONS 3/8 RULE OR A
C             COMBINATION OF THESE TWO RULES. TRUNCATION ERROR IS OF
C             ORDER H**5 (I.E. FOURTH ORDER METHOD). ONLY IN CASE NDIM=3
C             TRUNCATION ERROR OF Z(2) IS OF ORDER H**4.
C             FOR REFERENCE, SEE
C             (1) F.B.HILDEBRAND, INTRODUCTION TO NUMERICAL ANALYSIS,
C                 MCGRAW-HILL, NEW YORK/TORONTO/LONDON, 1956, PP.71-76.
C             (2) R.ZURMUEHL, PRAKTISCHE MATHEMATIK FUER INGENIEURE UND
C                 PHYSIKER, SPRINGER, BERLIN/GOETTINGEN/HEIDELBERG, 1963,
C                 PP.214-221.
C
C
C     ...............................................................
C
      SUBROUTINE QSF (H,Y,Z,NDIM)
C
C
      DIMENSION Y(1),Z(1)
C
      HT=.3333333*H
      IF(NDIM-5)7,8,1
C
C     NDIM IS GREATER THAN 5. PREPARATIONS OF INTEGRATION LOOP
    1 SUM1=Y(2)+Y(2)
      SUM1=SUM1+SUM1
      SUM1=HT*(Y(1)+SUM1+Y(3))
      AUX1=Y(4)+Y(4)
      AUX1=AUX1+AUX1
      AUX1=SUM1+HT*(Y(3)+AUX1+Y(5))
      AUX2=HT*(Y(1)+3.875*(Y(2)+Y(5))+2.625*(Y(3)+Y(4))+Y(6))
      SUM2=Y(5)+Y(5)
      SUM2=SUM2+SUM2
      SUM2=AUX2-HT*(Y(4)+SUM2+Y(6))
```

30

```
      Z(1)=0.
      AUX=Y(3)+Y(3)
      AUX=AUX+AJX
      Z(2)=SUM2-HT*(Y(2)+AUX+Y(4))
      Z(3)=SUM1
      Z(4)=SUM2
      IF(NDIM-F)5,5,2
C
C     INTEGRATION LOOP
    2 DO 4 I=7,NDIM,2
      SUM1=AJX1
      SUM2=AUX2
      AUX1=Y(I-1)+Y(I-1)
      AUX1=AUX1+AUX1
      AUX1=SUM1+HT*(Y(I-2)+AUX1+Y(I))
      Z(I-2)=SUM1
      IF(I-NDIM)3,6,6
    3 AUX2=Y(I)+Y(I)

      AUX2=AUX2+AJX2
      AUX2=SUM2+HT*(Y(I-1)+AUX2+Y(I+1))
    4 Z(I-1)=SUM2
    5 Z(NDIM-1)=AJX1
      Z(NDIM)=AJX2
      RETURN
    6 Z(NDIM-1)=SJM2
      Z(NDIM)=AJX1
      RETURN
C     END OF INTEGRATION LOOP
C
    7 IF(NDIM-7)12,11,8
C
C     NDIM IS EQUAL TO 4 OR 5
    8 SUM2=1.125*HT*(Y(1)+Y(2)+Y(2)+Y(2)+Y(3)+Y(3)+Y(3)+Y(4))
      SUM1=Y(2)+Y(2)
      SUM1=SUM1+SUM1
      SUM1=HT*(Y(1)+SUM1+Y(3))
      Z(1)=0.
      AUX1=Y(3)+Y(3)
      AUX1=AUX1+AJX1
      Z(2)=SUM2-HT*(Y(2)+AUX1+Y(4))
      IF(NDIM-5)10,9,9
    9 AUX1=Y(4)+Y(4)
      AUX1=AUX1+AUX1
      Z(5)=SUM1+HT*(Y(3)+AUX1+Y(5))
   10 Z(3)=SUM1
      Z(4)=SUM2
      RETURN
C
C     NDIM IS EQUAL TO 3
   11 SUM1=HT*(1.25*Y(1)+Y(2)+Y(2)-.25*Y(3))
      SUM2=Y(2)+Y(2)
      SUM2=SUM2+SJM2
      Z(3)=HT*(Y(1)+SUM2+Y(3))
      Z(1)=0.
      Z(2)=SUM1
   12 RETURN
      END
```

31